From Thermal Phase Transitions to Gauge Extensions

Optimising gravitational-wave signals in $U(1)$ models

Miguel Alcaraz Osorio

Supervision: António de Aguiar e Pestana de Morais

LIP Summer Internship ▪ 03-09-2026

The CFF potential drives the transition

ϕ is the order parameter, and temperature reshapes its free-energy landscape.

$$V(\phi, T) = \frac{\gamma}{2}(T^2 - T_0^2)\phi^2 - \frac{A}{3}T\phi^3 + \frac{\lambda}{4}\phi^4.$$

Thermal mass

Favours the symmetric state $\phi = 0$ at high temperature.

Cubic barrier

Separates the two phases, allowing a first-order transition.

Quartic stability

Bounds the potential at large field values.

Cooling changes the balance between these terms, reshaping the potential and enabling the transition.

Cooling produces expanding bubbles

$T > T_{\rm ext}$	$T_{\rm ext} > T > T_c$	$T = T_c$	$T_c > T > T_n$	$T = T_n$	$T = T_p$
one minimum	second minimum	equal phases	false vacuum	nucleation	percolation

No bubbles yet

Before T_n, the background still fills space.

Benchmark 3 used in the next five potential plots

$$\gamma = 1/9, \quad A = \sqrt{10}/144, \quad \lambda = 1.25/648, \quad T_0 = 140\ \mathrm{GeV}$$
$$T_{\rm ext} = 211.66\ \mathrm{GeV}, \quad T_c = 197.99\ \mathrm{GeV}, \quad T_n = 148.03\ \mathrm{GeV}, \quad T_p = 147.18\ \mathrm{GeV}$$

At high temperature, symmetry is restored

$T > T_{\rm ext} \;\rightarrow\; T_{\rm ext} > T > T_c \;\rightarrow\; T = T_c \;\rightarrow\; T_c > T > T_n \;\rightarrow\; T = T_n \;\rightarrow\; T = T_p$

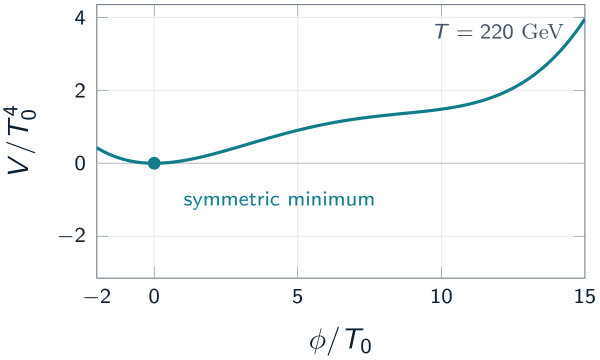

Physical picture

Positive thermal mass:
$m^2_{\rm eff}(T) = \gamma(T^2 - T_0^2) > 0.$

Only one minimum: $\phi = 0$.

No bubbles: no competing phase exists yet.

A second minimum forms

$T > T_{\text{ext}} \rightarrow T_{\text{ext}} > T > T_c \rightarrow T = T_c \rightarrow T_c > T > T_n \rightarrow T = T_n \rightarrow T = T_p$

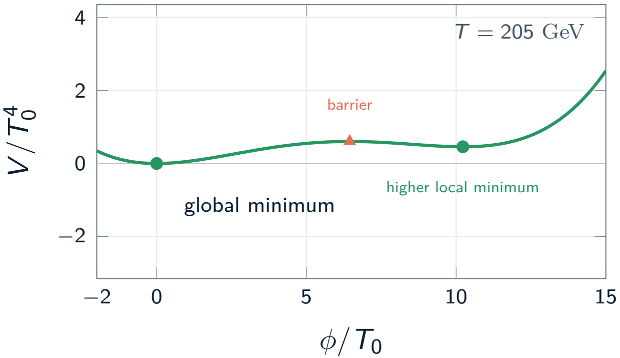

New extrema

- At $T_{\text{ext}} = 211.66$ GeV, a maximum–minimum pair first appears.
- For $T_{\text{ext}} > T > T_c$, the non-zero minimum is still higher.
- The symmetric phase remains globally preferred.

The barrier exists before phase degeneracy.

At T_c, the phases are degenerate

$T > T_{\rm ext} \;\to\; T_{\rm ext} > T > T_c \;\to\; T = T_c \;\to\; T_c > T > T_n \;\to\; T = T_n \;\to\; T = T_p$

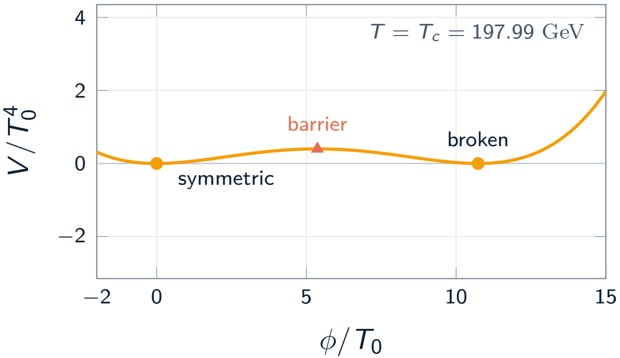

Degenerate minima

$V(0, T_c) = V(\phi_b, T_c)$.

- Equal free energy.
- Different order parameter.
- A barrier separates the phases.

T_c means coexistence, not nucleation or completion.

Supercooling below T_c

$$T > T_{\rm ext} \rightarrow T_{\rm ext} > T > T_c \rightarrow T = T_c \rightarrow T_c > T > T_n \rightarrow T = T_n \rightarrow T = T_p$$

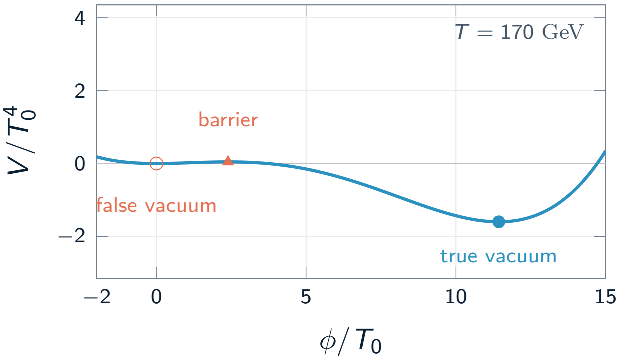

Metastable phase

- The broken minimum is deeper: $\Delta V < 0$.
- The origin is still a local minimum.
- The field remains trapped by the barrier.

This metastable delay is supercooling.

At T_n, critical bubbles nucleate

$T > T_{\rm ext} \;\to\; T_{\rm ext} > T > T_c \;\to\; T = T_c \;\to\; T_c > T > T_n \;\to\; T = T_n \;\to\; T = T_p$

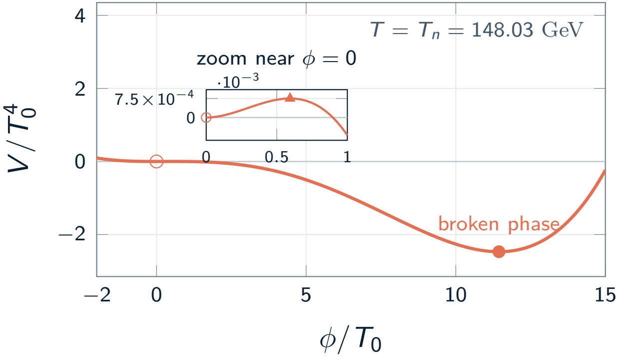

What changes at T_n?

1. The barrier is still present.
2. Cooling makes thermal tunnelling less suppressed.
3. Critical bubbles begin to form, but the transition is not yet complete.

At T_p, bubbles connect

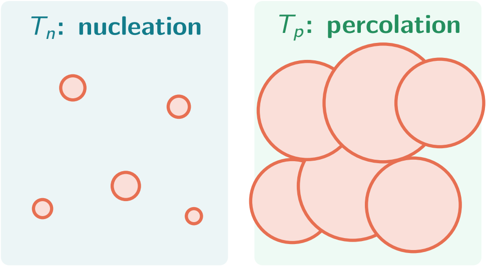

isolated critical bubbles

a connected broken-phase network forms

Percolation

$$I(T_p) = 0.34$$

$$P_{\rm FV}(T_p) = e^{-I(T_p)} \simeq 0.71$$

$$f_{\rm conv}(T_p) = 1 - P_{\rm FV}(T_p) \simeq 0.29$$

About 29% of space has converted: enough for the bubbles to connect.

Benchmark 3: $T_* = T_p = 147.18\ \mathrm{GeV}.$

Completion is a separate test: $\frac{\mathrm{d}}{\mathrm{d}t}(a^3 P_{\rm FV}) < 0.$ The physical false-vacuum volume must shrink despite cosmic expansion.

Three quantities shape the GW spectrum

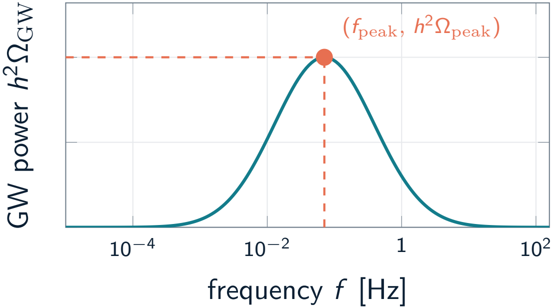

$T_* = T_p$

Energy scale and redshift $\Rightarrow$ peak frequency.

α

Released energy relative to radiation $\Rightarrow$ source power.

β/H_*

Inverse duration $\Rightarrow$ peak frequency and amplitude.

$$(T_*, \alpha, \beta/H_*) \implies (f_{\rm peak}, h^2\Omega_{\rm peak})$$

Four detectors, four frequency bands

SKA
nanohertz

LISA
millihertz

BBO
decihertz

ET
tens to hundreds of hertz

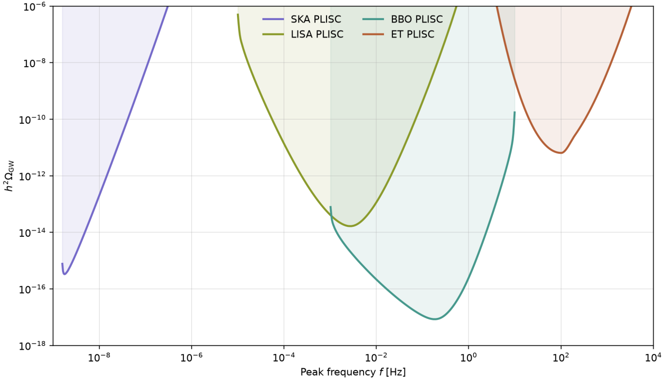

Crossing a sensitivity curve indicates projected reach, not a detection.

CFF+c adds one new barrier scale

$$V_c(\phi, T) = \frac{\gamma}{2}(T^2 - T_0^2)\phi^2 - \frac{AT + c}{3}\phi^3 + \frac{\lambda}{4}\phi^4.$$

The replacement $AT \longmapsto AT + c$ adds a temperature-independent cubic contribution.

The dimensionless shape coordinate is

$$r_C = \frac{c}{AT_0}.$$

$c = 0$ is exactly the CFF model.

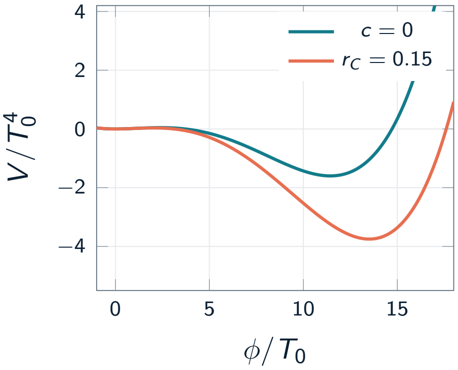

DAH introduces a charged dark scalar

A charged complex scalar $S = s/\sqrt{2}$ lives in a hidden $U(1)'$:

$$V_0(s) = -\frac{1}{2}\mu^2 s^2 + \frac{\lambda_S}{8} s^4, \qquad \mu^2 = \frac{\lambda_S}{2} v_{S0}^2.$$

$$\langle s \rangle = v_{S0}, \qquad m_{A'} = g_D v_{S0}.$$

The VEV breaks $U(1)'$ and gives the dark gauge boson a mass.

g_D: gauge coupling; λ_S: scalar coupling;
v_{S0}: zero-temperature scale.

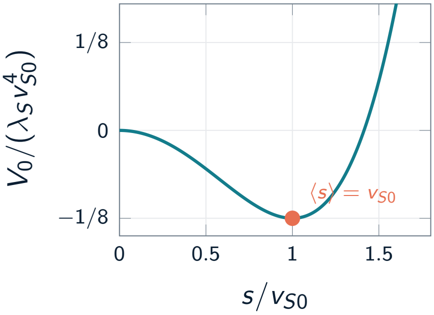

Quantum loops preserve the DAH vacuum

Masses in the loop sum

$$m_s^2(s) = -\mu^2 + \frac{3}{2}\lambda_S s^2,$$
$$m_G^2(s) = -\mu^2 + \frac{1}{2}\lambda_S s^2,$$
$$m_{A_i}^2(s) = g_D^2 s^2, \qquad i = 1, 2, 3.$$

These masses are evaluated on the background s; V_0 was defined on the previous slide.

Coleman–Weinberg contribution

$$V_{\rm CW}^{\rm bare}(s) = \frac{1}{64\pi^2}\sum_i m_i^4(s)\left[\ln\left(\frac{|m_i^2(s)|}{\Lambda^2}\right) - c_i\right].$$

$$V_{\rm CW}(s) = V_{\rm CW}^{\rm bare}(s) - \frac{1}{2}\delta\mu^2 s^2 + \frac{\delta\lambda}{8}s^4.$$

$c_i = 3/2$ for scalar modes, $c_i = 5/6$ for gauge modes, and the reference scale is $\Lambda = v_{S0}$.

$V'_{\rm CW}(v_{S0}) = V''_{\rm CW}(v_{S0}) = 0$: **the counterterms keep the input VEV and radial curvature unchanged.**

The full thermal function defines V_T

Finite-temperature contribution

$$V_T(s, T) = \frac{T^4}{2\pi^2} \sum_i J_B\left(\frac{m_i^2(s)}{T^2}\right),$$

$$J_B(\theta) = \mathrm{Re}\int_0^\infty dx\, x^2 \ln\left[1 - e^{-\sqrt{x^2+\theta}}\right].$$

What the search varies

$$(g_D, \lambda_S, v_{S0}, \xi)$$

$$\xi = \frac{T_{\rm hidden}}{T_{\rm SM}}.$$

The temperature ratio changes the expansion rate, redshift, transition strength and observed frequency.

The numerical stages evaluate J_B directly; a high-temperature polynomial never certifies a transition.

Daisy resummation regulates zero modes

Arnold–Espinosa contribution

$$V_{\rm Daisy}(s,T) = -\frac{T}{12\pi}\sum_i \left([m_i^2(s)+\Pi_i(T)]_+^{3/2} - [m_i^2(s)]_+^{3/2}\right),$$

$$\Pi_s = \Pi_G = \left(\frac{\lambda_S}{6}+\frac{g_D^2}{4}\right)T^2.$$

$$\Pi_{A_L} = \frac{g_D^2}{3}T^2, \qquad \Pi_{A_T} = 0.$$

where $[x]_+ = \max(x,0)$. The thermal masses resum the infrared-sensitive bosonic zero modes.

$$\boxed{V_{\rm eff}(s,T) = V_0(s) + V_{\rm CW}(s) + V_T(s,T) + V_{\rm Daisy}(s,T)}$$

All broad, screening and strict calculations use this complete potential.

The program is a funnel: explore cheaply, validate carefully

many parameter guesses → fast broad checks → numerical screening → detector-guided refinement → strict recalculation → validated atlas

Search stages decide where to spend time

- cover large continuous parameter ranges;
- move promising scales toward detector bands;
- refine useful placements.

The strict stage decides what is kept

- solve the bubble profile again at higher resolution;
- require nucleation, percolation and completion;
- save checkpoints and reproducible collections.

Each dot is one transition that survived the full physical chain

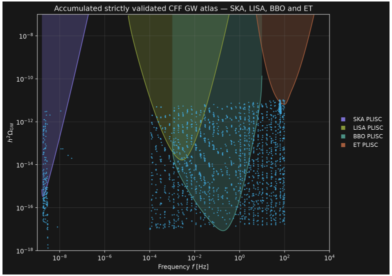

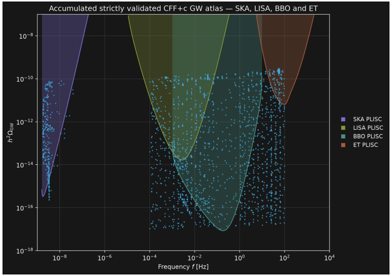

CFF: controlled baseline

Dense LISA–ET coverage plus a strict SKA population.

CFF+c: one extra shape coordinate

Wider SKA–ET coverage, with exact $c = 0$ controls.

Dots are validated spectra; coloured curves are detector reach references. Density reflects sampling, not probability.

The gauge model also produces signals across detector bands

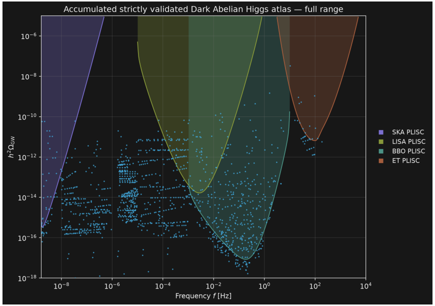

What is different?

Gauge and scalar thermal loops reshape the barrier.

What is the same?

Continuous search and a fresh strict calculation for every dot.

DAH maps reveal scale and strength

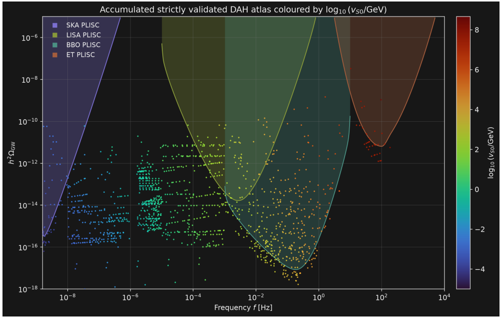

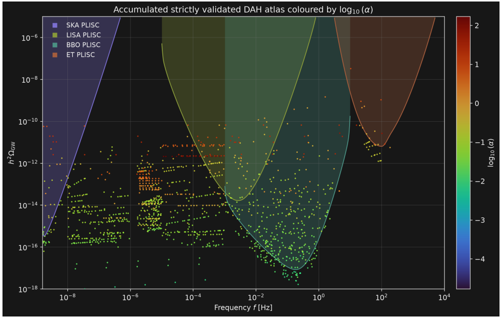

Scale chain: v_{S0} changes the computed T_p, moving the peak horizontally.

Transition strength: α tracks how much released energy can feed the source.

The code is built for robustness: every plotted point passes a fresh strict bounce, percolation and completion calculation.

Transition duration in Hubble units

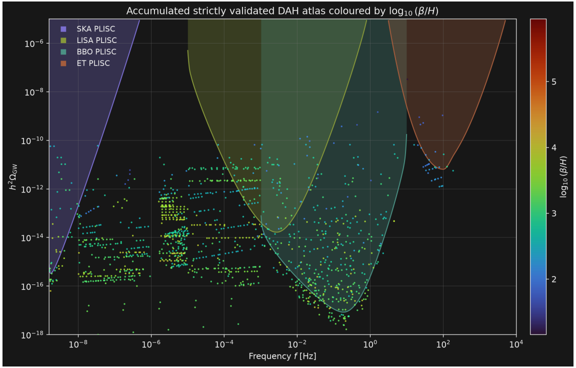

Two physical clocks

$$\Delta t_{\rm PT} \sim \beta^{-1}, \quad t_H = H_*^{-1}$$

$$\frac{\beta}{H_*} \sim \frac{t_H}{\Delta t_{\rm PT}}$$

Small β/H_*

Longer transition

$\Downarrow\ f_{\rm peak} \qquad \Uparrow\ \Omega_{\rm GW}$

Large β/H_*

Faster transition

$\Uparrow\ f_{\rm peak} \qquad \Downarrow\ \Omega_{\rm GW}$

Trends at fixed T_*, α and wall velocity.

The physical story and the software now meet in one atlas

Physical mechanism

Cooling $\rightarrow$ bubbles $\rightarrow$ plasma sound waves $\rightarrow$ GW background.

Software contribution

Explore widely, target detector bands and strictly validate every saved point.

Scientific result

All three models populate the conditional SKA–ET atlas; CFF+c and DAH test additional physics.

Central lesson: a large peak is not enough; the transition must occur, complete and remain stable.

Questions?